Accepted for Earth and Planetary Science Letters 31.10.2017

Reply to the Comment on "Astronomical constraints on the duration of the Early Jurassic Pliensbachian Stage and global climatic fluctuations" (Ruhl et al., Earth and Planetary Science Letters, 455 (2016) 149–165)

Linda A. Hinnov[1], Micha Ruhl[2], Stephen P. Hesselbo[3]

[1] Department of Atmospheric, Oceanic, and Earth Sciences, George Mason University, Fairfax, Virginia 22030 USA
[2] Department of Earth Sciences, University of Oxford, South Parks Road, OX13AN, Oxford, UK
[3] Camborne School of Mines and Environment and Sustainability Institute, Exeter University, Penryn Campus, Penryn Cornwall TR10 9FE, UK

Introduction

Smith and Bailey (2017) (henceforth SB17) criticize methods employed in our recent study of a highly cyclic calcium (Ca) series measured through the Early Jurassic, Pliensbachian-age, marine succession of the Llanbedr (Mochras Farm) core, referred to as Mochras (Ruhl et al., 2016, henceforth R16). In particular SB17 focus on the red noise spectral models calculated in R16. Here we clarify the red noise models displayed in Figure 5 and Supplementary Figures 4 and 5 of R16, and comment further on estimating power spectra and AR1 red noise model spectra. We highlight effects from nonrandom data variation, sampling and pre-whitening on red noise model estimation, and concur with SB17 that red noise modeling should not be applied with a "boiler-plate" approach. Using the Mochras Ca series as an example, we discuss practical solutions that can be used for other cyclostratigraphic data presenting similar issues. In summary, whereas SB17 advocate alternative red noise models, e.g., bent power law models, we show that modest adjustments to the data can dramatically improve the fit between AR1 red noise and data spectra.

Red noise spectra in R16

The red noise spectra in Supplementary Figures 4 and 5 of R16 were calculated according to the conventional AR1 red noise model computed by the "mtm" function in the Astrochron package for R (Meyers, 2014). The supplementary figures therefore include "AR1 Confidence Level Estimates," which are exclusively the output of "mtm". Only the conventional AR1 red noise spectrum is displayed; confidence levels with respect to the Ca data spectrum were not included (e.g. 90%, 95% and 99%). The red noise spectrum displayed in Figure 5 of R16 is based on the robust AR1 red noise model (Mann and Lees, 1996), and was computed with the "mtmML96" function in Astrochron.

The conventional AR1 red noise model

As discussed elsewhere (Meyers, 2012) the conventional AR1 red noise spectral model can be severely biased. The biasing can be either low or high depending on the frequency distribution of nonrandom signal and random noise in the data, and on data sampling rate, which affects calculation of the lag-1 autocorrelation coefficient (ρ) of the data that is used in the AR1 model. In both Supplementary Figures 4 and 5 of R16, the conventional AR1 red noise spectra appear to be overestimated at low frequencies, and underestimated at middle to high frequencies, where multiple data spectral peaks greatly exceed even the 99% CL.

One challenge relates to the effect of high-amplitude, very low frequencies in data. The Ca series is affected by a ~150-meter-long cycle, which adversely affects the computation of both the data power spectrum and the AR1 red noise spectrum (e.g., Supplementary Figure 4A of R16). The removal of this variation by high-pass filtering is key to evaluating the other nonrandom spectral components of the Ca series. This was carried out using the notch filter option in Analyseries 2.0.8, setting the center frequency at 0.0 and the cut-off frequency at 1/(150 m); the results are displayed in Figure 4A ("detrended Ca series") of R16. (SB17 elected to remove a 5th order polynomial fit from the Ca series for their analyses.)

A second challenge is that the stratigraphic series has a strong and persistent Ca cycle that occurs at a thickness of ~1 m, with variable sedimentation rates modulating this thickness from cycle to cycle along the series (see examples in Figures 3 and 4 of R16). The result is that in the stratigraphic spectrum of the entire Ca series, a broad frequency band is generated with elevated power centered at 1 cycle/m, with many spectral peaks (Supplementary Figure 4A of R16). The Geologic Time Scale 2012 (Ogg and Hinnov, 2012) indicates an ~8.1 million-year duration for the ~400-m-long Pliensbachian series, and so these ~1-m-thick cycles are precessional in scale. Removing the effects of the variable sedimentation rates should "snap" these cycles into narrow bands associated with precession index frequencies. To a certain extent this was accomplished by R16's 405-kyr tuning procedure, which produced a power spectrum with only a few elevated spectral peaks in the precession index band (Figure 5 of R16).

A third challenge is related to the sampling of the Ca series, which was set at an average of $\Delta d=0.12$ m in order to obtain a robust 8 samples per 1 m cycle (a standard originally suggested by Herbert, 1994). Unfortunately, this protocol has generated an especially undesirable effect in the calculation of ρ in the AR1 red noise spectrum model; this effect – and its management – is illustrated further below.

The robust AR1 red noise model

Robust AR1 red noise modeling involves a "pre-whitening" approach to reduce contributions from nonrandom signal at all frequencies when calculating the red noise spectrum (Mann and Lees, 1996). A "median smoothed background" estimation of the data spectrum is fitted to average noise level and ρ parameters while rejecting frequencies with excessive high power (presumed nonrandom signal). Hinnov et al. (2016) illustrated the difference between conventional and robust AR1 red noise spectra computed on a uniformly sampled AR1 red noise time series with $\rho = 0.7$. The elevated spectral peak near $f = 0$ (Figure 1A in Hinnov et al., 2016) and its rejection from the robust model is the likely cause for the large difference between the two AR1 models at low frequencies.

The robust AR1 red noise algorithm was recently improved in Astrochron's "mtmML96" to control edge effects and reduce false positive rates at low frequencies up to ~50% (Meyers, 2014), and was used to compute the robust AR1 red noise model for the 405-kyr tuned Fe time series in Figure 5 of R16.

Fit of red noise model spectrum to data spectrum

One of the objections of SB17 is that the AR1 red noise model spectrum (conventional or robust) does not adequately fit the Ca data spectrum; their criterion for a good or poor fit is limited to visual inspection. In REDFIT (Schulz and Mudelsee, 2002) a "non-parametric runs test" is performed to evaluate the fit of the conventional AR1 red noise spectrum to the data spectrum. This test has not yet been strongly emphasized as an important step in developing appropriate red noise models, and is not yet available in other cyclostratigraphic toolboxes (e.g. Astrochron). As with SB17, the following discussion relies on visual comparisons; ultimately all of these comparisons should be evaluated statistically with a procedure such as that provided in REDFIT (and yet to be developed).

Sampling

Figure 1 demonstrates the effect of data sampling on the calculation of ρ, which is integral to the AR1 red noise model (conventional or robust), using the "mtm" and "mtmML96" functions in Astrochron. For input to multitaper spectral analysis, the Ca 405-kyr tuned time series was linearly interpolated to a uniform sample rate of $\Delta t = 0.41$ kyr, i.e. the median sample rate of the time-converted series. The results for the entire Nyquist range (0 to $1/(2\cdot 0.41$ kyr$)=1.22$ cycles/kyr) reveal a considerable and obvious misfit between data and conventional AR1 red noise spectra (**Figure 1A**). There are shallow notches that characterize the data spectrum at regular intervals (f=0.0003, 0.004, 0.015, 0.09 and 0.25), and the highest frequencies (>0.3 cycles/kyr) take on an aspect of very high variability. This plot can be compared with the Ca power spectral analysis shown in Supplementary Figure 5 of R16, although that analysis used 3π multitapers. Only one low frequency spectral peak at 1/(101.8 kyr) exceeds the 99% CL; many peaks in the high frequencies lie far above the 99% CL. Below we offer a solution to this highly biased result that points directly to the original sampling protocol.

An alternative lower uniform sample rate of $\Delta t = 6.0$ kyr sets the Nyquist frequency to a much lower value of $1/(2\cdot 6$ kyr$) = 0.08333$ cycles/kyr, and provides a more reasonable fit between data spectrum and conventional AR red noise spectrum (**Figure 1B**). Other (smaller) Δt's were also tested; $\Delta t = 6.0$ kyr was the largest and thus closest to the precession band, but still guaranteeing 3 to 4 samples per precession cycle. The shallow notches in this version of the data spectrum divide the spectrum into bands that coincide with the long orbital eccentricity, short orbital eccentricity, and obliquity and precession (E, e, and O-p). In the Milankovitch band, multiple spectral peaks exceed the 99% CL; in particular the two peaks with periodicities at 136.8 kyr and 101.8 kyr are close to the short orbital eccentricity periods of 127 kyr and 97 kyr.

The fact that simple 405-kyr tuning restricted so much power into these narrow frequency bands is powerful evidence for the presence of Milankovitch forcing.

Robust AR1 red noise modeling is clearly indicated by the evidence for nonrandom signal, and results for the $\Delta t = 6.0$ kyr sampled Ca time series are shown for two versions of robust AR1 red noise (**Figures 1C, 1D**). The first version calculates the median smoothed background spectrum with linear power (linlog=1). This is recommended for data spectra with a broad frequency distribution of power (Mann and Lees, 1996). For data spectra with a "high dynamic range" and with most power concentrated in the low frequencies, median smoothing with log power (linlog=2) is recommended. Mann and Lees (1996) also warn that significance estimates that are strongly dependent on linear versus log fitting "should not be interpreted with great confidence." In this case, the spectral peaks at 16.0 kyr and 14.8 kyr fall into the low confidence category. Finally, the window size of the median smoothing is recommended to be 20% of the Nyquist frequency, but this is adjustable as well. However, the wider the smoothing window, the more likely that low power high frequencies will bias the result.

Discussion

SB17 raise their objections from the very start, challenging the significance of the "5.8 m" spectral peak in the raw Ca stratigraphic spectrum, which falls short of any CL level in their Figure 1A. To be conformable with GTS2012, the 5.8 m cycle is short orbital eccentricity (~100 kyr) scale, which is the astronomical parameter that cannot be measured adequately in the spectral domain, and is especially prone to failing spectral significance tests (Meyers, 2012). This is because short orbital eccentricity cycles strongly modulate in frequency and amplitude through time; power is divided into 2 major bands that themselves are bifurcated (see Figure 4.3 in Hinnov and Hilgen, 2012). This problem is only compounded by the added variable sedimentation rates and other post-depositional processes that affect cyclostratigraphy. Instead, R16 focused on ~25 m cycles to select 405 kyr intervals, represented by a spectral peak that exceeds the 95% CL in Figure 1A of SB17.

The argument then hinges on the proper definition of confidence level, but prior to deciding that, the most appropriate red noise model needs to be identified. SB17 conclude that the most appropriate red noise model for the Mochras Ca stratigraphic series is a bent power law model, but a lower-sampled Ca stratigraphic series may provide an equally valid AR1 red noise model.

Figure 2 replicates and extends the analysis provided in Figure 1A of SB17. Here we apply 2π MTM power spectral analysis; while it is not stated, SB17 appear to use 3π MTM power spectra which has a broader frequency band resolution. Consequently, SB17 were not able to resolve most of the low frequencies, which the 2π resolution readily identifies with wavelengths exceeding the 99% CL at 74 m, 34 m, and 25 m. Robust red noise modeling with median smoothing using linear power even sets the now well-resolved 6.0 m cycle above the 99% CL (**Figure 2A**). However, for the median-sampled (Δd=0.12 m) Ca stratigraphic series, the highest frequencies diverge from the robust red noise model (red arrow, **Figure 2A**), although not quite to the extent reported in SB17, probably due to the difference in 2π vs. 3π multiapers used for the data spectrum. SB17 also do not indicate how the robust autocorrelation coefficient ρ was determined, nor do they indicate whether they used linear or log power for calculating the median smoothed background in any of their analyses.

Again, we demonstrate the effect of sampling on AR1 red noise modeling, together with robust red noise models using linear vs. log power-based background spectrum estimation (**Figures 2B** and **2C**). Doubling the data sample rate both raises the AR1 red noise model, and changes its shape in the high frequencies, showing an improved fit (red arrow, **Figure 2B**). The elevated noise now slightly reduces the significance of the 6.0 m spectral peak (to below the 99% CL); log power fitting of the background spectrum further reduces the 6.0 m peak significance, as well as improving the fit of the model to data in the high frequencies (red arrow, **Figure 2C**). As to correction of the CLs to account for "multiple tests of significance" solution proposed by SB17 is not realistic, especially in light of the limited frequency bands of interest (Hinnov et al. 2016) and the simple sampling reduction illustrated here, among other factors (variable sedimentation rates).

The adjustments we have suggested above indicate that straight away rejection of AR1 red noise modeling is unwarranted, at least in this case. Moreover, the misfit of data spectra to noise spectra can lead to new hypotheses about natural processes, and as demonstrated here, new protocols for data collection and data treatment. That said, the spectral background structure of cyclostratigraphy remains an unexplored subject that would benefit greatly from future study.

References

Herbert, T.D., 1994. Reading orbital signals distorted by sedimentation: models and examples. In: De Boer, P. and Smith, D.G., eds., Orbital Forcing and Cyclic Sequences, Special Publications of the International Association of Sedimentologists, 19, 483-507.

Hinnov, L.A., Wu, H., and Fang, Q. (2016), Reply to the comment on "Geologic evidence for chaotic behavior of the planets and its constraints on the third-order eustatic sequences at the end of the Late Paleozoic Ice Age" by Qiang Fang, Huaichun Wu, Linda A. Hinnov, Xiuchun Jing, Xunlian Wang, and Qingchun Jiang [Palaeogeography Palaeoclimatology Palaeoecology 400 (2015) 848–859], Palaeogeography Palaeoclimatology Palaeoecology, 461, 475-480, doi:10.1016/j.palaeo.2016.07.030

Hinnov, L.A., and Hilgen, F., 2012. Chapter 4: Cyclostratigraphy and Astrochronology, in Gradstein, F.M., Ogg, J., Schmitz, M., and Ogg, G., eds., The Geologic Time Scale 2012, Elsevier, 63-83, doi: 10.1016/B978-0-444-59425-9.00004-4

Mann, M.E., Lees, J.M., 1996. Robust estimation of background noise and signal detection in climatic time series. Climatic Change, 33, 409–445.

Meyers, S.R., 2012. Seeing red in cyclic stratigraphy: spectral noise estimation for astrochronology. Paleoceanography 27, PA3228, doi:10.1029/2012PA002307.

Meyers, S.R., 2014. Astrochron: an R package for astrochronology. http://cran.rproject. org/package=astrochron.

Ogg, J.G. and Hinnov, L.A., 2012. Chapter 26: Jurassic. In: Gradstein, F.M, Ogg, J.G., Schmitz, M., and Ogg, G., eds., The Geologic Time Scale 2012, Elsevier, Amsterdam, 731-791, doi: 10.1016/B978-0-444-59425-9.00026-3

Ruhl, M., Hesselbo, S.P., Hinnov, L.A., Jenkyns, H.C., Xu, W., Storm, M., Riding, J., Minisini, D., Ullmann, C.U., and Leng, M.J. (2016), Astronomical constraints on the duration of the Early Jurassic Pliensbachian stage and global climate fluctuations, Earth and Planetary Science Letters, 455, 149-165, doi: 10.1016/j.epsl.2016.08.038

Schulz, M., and Mudelsee, M., 2002. REDFIT: estimating red-noise spectra directly from unevenly spaced paleoclimatic time series. Computers and Geosciences, 28, 421–426.

Smith, D.G., and Bailey, R.J., 2017. Comment on "Astronomical constraints on the duration of the Early Jurassic Pliensbachian Stage and global climatic fluctuations" (Ruhl et al., Earth and Planetary Science Letters, 455 (2016) 149-165), this issue.

Figure captions

Figure 1. 2π MTM power spectral analysis of the detrended (procedure of R16) Mochras 405-kyr tuned Ca time series with AR1 red noise modeling. Insets are linear plots of the Milankovitch band. All figures were created in MATLAB.

A. Ca time series interpolated to the median spacing Δt = 0.41 kyr, with conventional AR1 red noise model spectrum (ρ = 0.9916). The following R command was used with the astrochron library:

```
catimeintMTM_41=mtm(catimeintall41,tbw=2,ntap=NULL,padfac=10,demean=T,detrend
=F,siglevel=0.9,ar1=T,output=1,CLpwr=T,xmin=0,xmax=1/(2*6.0),pl=1,sigID=T,gen
plot=T,verbose=T)
```

B. Ca time series interpolated to Δt = 6.0 kyr, with conventional AR1 red noise spectrum (ρ = 0.3316). The following R command was used with the astrochron library:

```
catimeintMTM_6=mtm(catimeintall6,tbw=2,ntap=NULL,padfac=10,demean=T,detrend=F
,siglevel=0.9,ar1=T,output=1,CLpwr=T,xmin=0,xmax=1/(2*6.0),pl=1,sigID=T,genpl
ot=T,verbose=T)
```

C. Ca time series interpolated to Δt = 6.0 kyr, with robust AR1 red noise spectrum computed with a median smoothing window of 0.2 x Nyquist using linear power and a grid search, and padding the data spectrum by a factor of 10. Robust ρ = 0.243. The following R command was used with the astrochron library:

```
catimeintML96_6_1=mtmML96(catimeintall6,tbw=2,ntap=NULL,padfac=10,demean=T,de
trend=F,medsmooth=0.2,opt=3,linLog=1,siglevel=0.9,output=1,CLpwr=T,xmin=0,xma
x=1/(2*6.0),sigID=T,pl=1,genplot=T,verbose=T)
```

D. Ca time series interpolated to Δt = 6.0 kyr, with robust AR1 red noise spectrum computed with a median smoothing window of 0.2 x Nyquist using log power and a grid search, and padding the data spectrum by a factor of 10. Robust ρ = 0.304. The following R command was used with the astrochron library:

```
(catimeintML96_6_1=mtmML96(catimeintall6,tbw=2,ntap=NULL,padfac=10,demean=T,d
etrend=F,medsmooth=0.2,opt=3,linLog=2,siglevel=0.9,output=1,CLpwr=T,xmin=0,xm
ax=1/(2*6.0),sigID=T,pl=1,genplot=T,verbose=T)
```

Figure 2. 2π MTM power spectral analysis of the detrended (procedure of SB17) Mochras Ca stratigraphic series with AR1 red noise modeling. All figures were created in MATLAB.

A. Ca stratigraphic series interpolated to the uniform median spacing Δd=0.12 m, with robust AR1 red noise model spectrum with linear power median spectral background fitting with a window of 0.2 x Nyquist and a grid search (conventional ρ= 0.7615427, robust ρ= 0.662). The following R command was used with the astrochron library:

```
carawintmtmML961=mtmML96(carawint,tbw=2,ntap=NULL,padfac=10,demean=T,detrend=F,medsmooth=0.2,opt=3,linLog=1,siglevel=0.9,output=1,CLpwr=T,xmin=0,xmax=1/(2*0.12),sigID=T,pl=1,genplot=T,verbose=T)
```

B. Ca stratigraphic series interpolated to a uniform spacing of Δd=0.24 m, with robust AR1 red noise model spectrum with linear power median spectral background fitting with a window of 0.2 x Nyquist and a grid search (conventional ρ= 0.4664586, robust ρ=0.395). The following R command was used with the astrochron library:

```
carawintnewmtmML961=mtmML96(carawintnew,tbw=2,ntap=NULL,padfac=10,demean=T,detrend=F,medsmooth=0.2,opt=3,linLog=1,siglevel=0.9,output=1,CLpwr=T,xmin=0,xmax=1/(2*0.24),sigID=F,pl=1,genplot=T,verbose=T)
```

C. Ca stratigraphic series interpolated to a uniform spacing of Δd=0.24 m, with robust AR1 red noise model spectrum with log power median spectral background fitting with a window of 0.2 x Nyquist and a grid search (conventional ρ= 0.4664586, robust ρ= 0.485). The following R command was used with the astrochron library:

```
carawintnewmtmML962=mtmML96(carawintnew,tbw=2,ntap=NULL,padfac=10,demean=T,detrend=F,medsmooth=0.2,opt=3,linLog=2,siglevel=0.9,output=1,CLpwr=T,xmin=0,xmax=1/(2*0.24),sigID=F,pl=1,genplot=T,verbose=T)
```

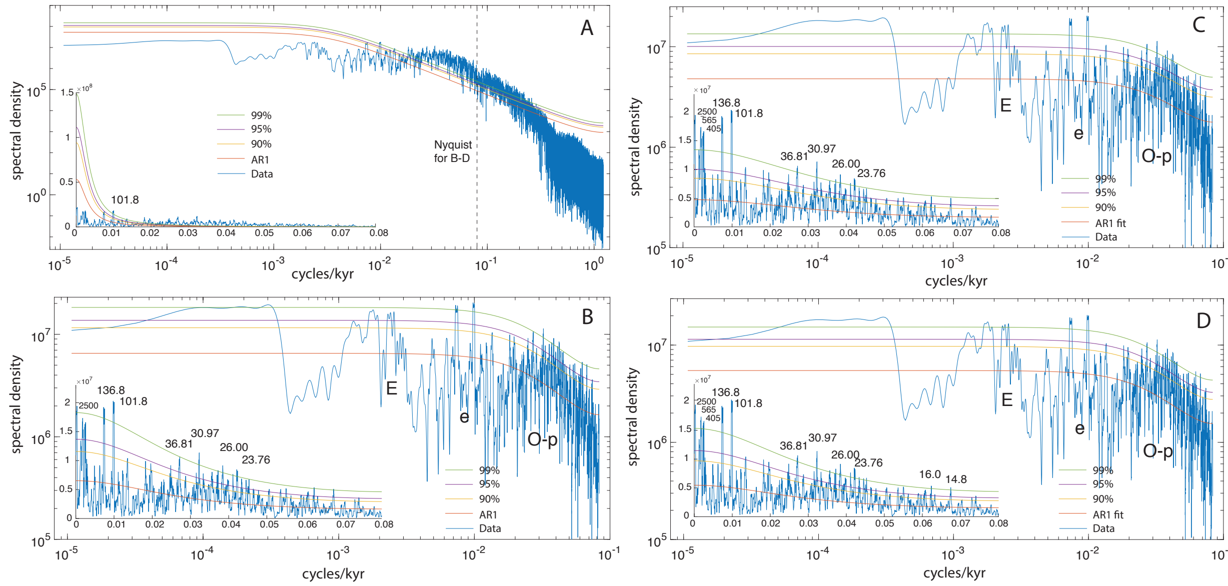
A
B
C
D
spectral density
cycles/kyr
Nyquist
for B-D
99%
95%
90%
AR1
AR1 fit
Data
101.8
136.8
2500
565
405
36.81
30.97
26.00
23.76
16.0
14.8
E
e
O-p

Figure 1

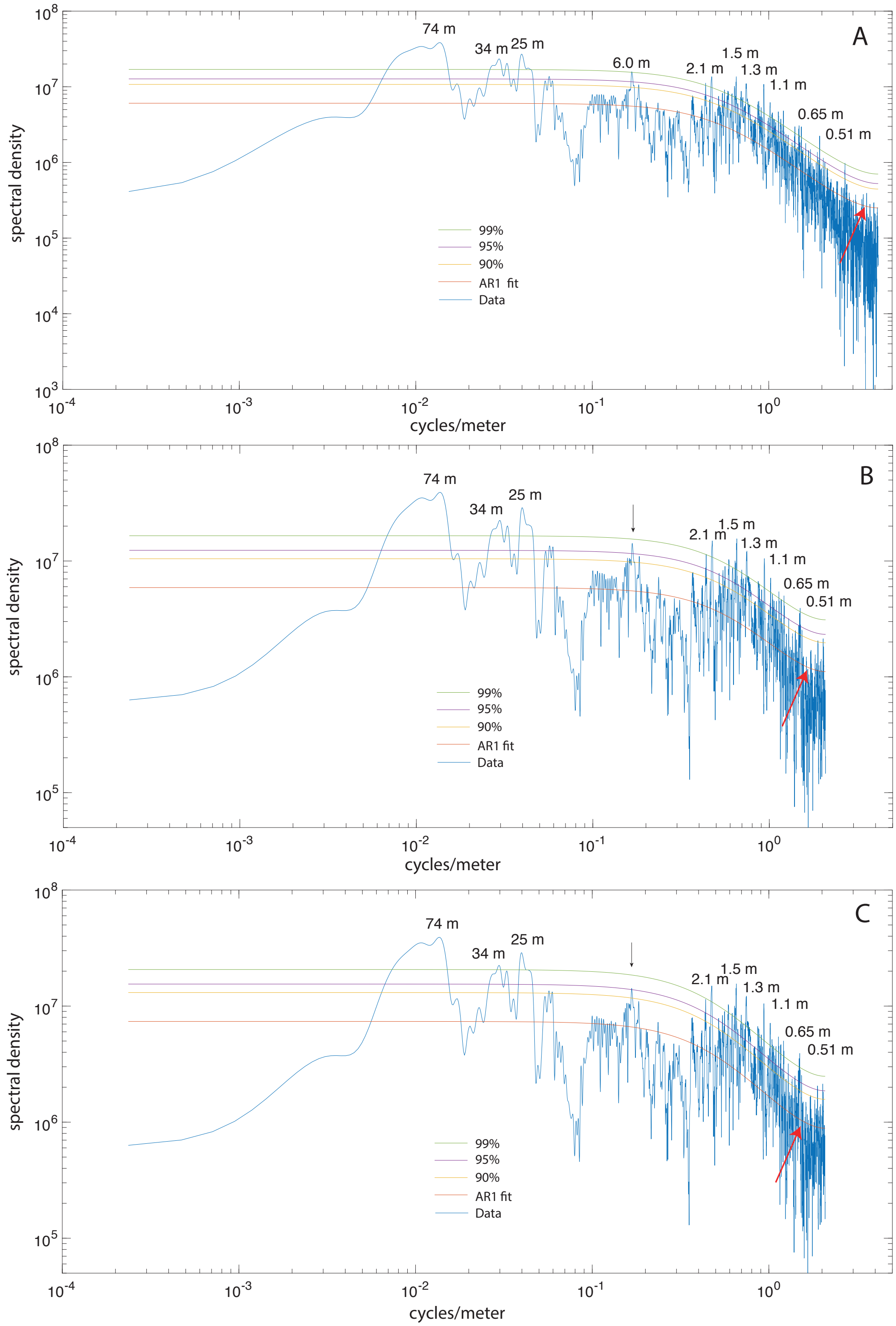

279

280 **Figure 2**